



CENTRO EURO-MEDITERRANEO  
PER I CAMBIAMENTI CLIMATICI



**CENTRO EURO-MEDITERRANEO PER  
I CAMBIAMENTI CLIMATICI**

ISC – Divisione Impatti sul Suolo e sulle Coste

Technical Reports

Final document on the third year,  
first activity:  
“Numerical techniques for  
preventing computational  
instability problems to simulate  
floods due to low-intensity  
rainfall”

**Prof. Francesco Macchione\***

**Ing. Pierfranco Costabile\***

**Ing. Carmelina Costanzo\***

*\* LAMPIT (Laboratorio di Modellistica numerica per la Protezione Idraulica del Territorio)  
– Dipartimento di Difesa del Suolo – Università della Calabria*

Centro Euro-Mediterraneo  
per i Cambiamenti Climatici  
[www.cmcc.it](http://www.cmcc.it)

May 2009 ■ TR



**Final document on the third year first activity: “Numerical techniques for preventing computational instability problems to simulate floods due to low-intensity rainfall”.**

Abstract

The purpose of the collaboration between LAMPIT (Department of Soil Defence, University of Calabria) and CMCC is to develop an hydrometeorological chain in order to obtain a reliable tool in the context of flood evolution prediction able to provide quantitative information of practical importance within the civil protection activities.

The LAMPIT contribution to the project concerns the mathematical description of both the generation and propagation of flood events at basin scale. The work here presented has been carried out in close cooperation with CIRA researchers (dr. Pasquale Schiano and dr. Paola Mercogliano). The evaluation in time and magnitude of the overland flow phenomena caused by rainfall is very important in a variety of environmental and hydraulics situations. The mathematical representation of the flow processes is based on the fully dynamic shallow water equations. The solution of these equations, excluding some simplified cases, can be obtained by numerical integration only. Many schemes based on fully dynamic and simplified shallow water equations have been proposed in literature. Some of these schemes are implemented in the LAMPIT laboratory and applied to simulate simple cases of overland flow as already presented. Afterwards the implemented codes have been applied to simulate overland flow over real topography. In this contest some numerical anomalies appear due to the presence of small water depth over high slope and irregular topography. In this work a careful analysis of these problems has been made and some numerical techniques have been implemented in order to prevent them.

The work has been organized as follows:

- Numerical schemes and techniques.
- Applications
- Numerical techniques for preventing computational instability problems

**Keywords:** Hydrometeorological chain, Flood propagation

**JEL Classification:**

*Address for correspondence:*

Prof. Francesco Macchione

Laboratorio LAMPIT

Dipartimento di Difesa del Suolo – Università della Calabria

Ponte P.Bucci – Cubo 42/B

87036, Rende (CS) .

E-mail: [f.macchione@unical.it](mailto:f.macchione@unical.it)



## NUMERICAL SCHEMES AND TECHNIQUES

In the previous report, according to a comparative analysis on numerical schemes, the MacCormack's scheme and HLL scheme have been improved and some numerical techniques have been implemented in order to simulate real overland flow situations.

The implemented codes are based on the fully conservative shallow water equations:

$$\frac{\partial \mathbf{U}}{\partial t} + \frac{\partial \mathbf{F}}{\partial x} + \frac{\partial \mathbf{G}}{\partial y} = \mathbf{S} \quad (1)$$

where:

$$\mathbf{U} = \begin{pmatrix} h \\ hu \\ hv \end{pmatrix} \quad (2)$$

$$\mathbf{F} = \begin{pmatrix} hu \\ hu^2 + gh^2/2 \\ huv \end{pmatrix}; \quad \mathbf{G} = \begin{pmatrix} hv \\ huv \\ hv^2 + gh^2/2 \end{pmatrix} \quad (3, 4)$$

$$\mathbf{S} = \begin{pmatrix} r - f \\ gh(S_{0x} - S_{fx}) \\ gh(S_{0y} - S_{fy}) \end{pmatrix} \quad (5)$$

with:

$t$  is time;  $x, y$  are the horizontal coordinates;  $h$  is the water depth;  $u, v$  are the depth-averaged flow velocity in  $x$ - and  $y$ - directions;  $g$  is the gravitational acceleration;  $S_{0x}, S_{0y}$  are the bed slopes in  $x$ - and  $y$ - directions;  $S_{fx}, S_{fy}$  are the friction slopes in  $x$ - and  $y$ - directions, which can be calculated from Strickler's formula as:

$$S_{fy} = \frac{v\sqrt{u^2 + v^2}}{K_s^2 h^{4/3}} \quad S_{fx} = \frac{u\sqrt{u^2 + v^2}}{K_s^2 h^{4/3}} \quad (6,7)$$

$r$  is the rain intensity and  $f$  are the infiltration losses.

The finite volume method, widely adopted in the literature, has been used to discretize the previous equations. It considers the integral form of the shallow water equations that allows a quite easy implementation of shock capturing schemes on different mesh type.

The system of equation is integrated over an arbitrary control volume  $\Omega_{i,j}$  and, in order to obtain surface integrals the application of Green's theorem to each component of the vectors  $\mathbf{F}$  and  $\mathbf{G}$  leads to (Hirsch, 1990):

$$\frac{\partial}{\partial t} \int_{\Omega_{i,j}} \mathbf{U} d\Omega + \oint_{\partial\Omega_{i,j}} [\mathbf{F}, \mathbf{G}] \cdot \mathbf{n} dL = \int_{\Omega_{i,j}} \mathbf{S} d\Omega \quad (8)$$



where  $\partial\Omega_{i,j}$  being the boundary enclosing  $\Omega_{i,j}$ ,  $\mathbf{n}$  is the unit vector normal and  $dL$  is the length of each boundary. Denoting by  $\mathbf{U}_{i,j}$  the average value of the flow variables over the control volume  $\Omega_{i,j}$  at a given time, the equation (8) may be discretized as:

$$\mathbf{U}_{i,j}^{n+1} = \mathbf{U}_{i,j}^n - \frac{\Delta t}{\Omega_{i,j}} \sum_{r=1}^4 [\mathbf{F}, \mathbf{G}]_r \cdot \mathbf{n}_r \Delta L_r + \Delta t \mathbf{S}_{i,j}^n \quad (9)$$

The finite volume method, as represented by the equation (8), allows the decomposition of a two dimensional problem into a series of locally one dimensional problems to value the normal flux through every side of a cell. Many algorithms have been proposed for the flux vectors evaluation: the most diffused in literature have been examined and implemented .

In the analysis presented herein the MacCormack second order space centered scheme and the first order upwind HLL scheme have been applied.

MacCormack's predictor-corrector scheme has an accuracy of second order in both space and time. The numerical integration of system (1) is performed in the following form:

$$\mathbf{U}_{i,j}^p = \mathbf{U}_{i,j}^n - \frac{\Delta t}{\Omega_{i,j}} \sum_{r=1}^4 [\mathbf{F}, \mathbf{G}]_r^n \cdot \mathbf{n}_r \Delta L_r + \Delta t \mathbf{S}_{i,j}^n \quad (10)$$

$$\mathbf{U}_{i,j}^c = \mathbf{U}_{i,j}^n - \frac{\Delta t}{\Omega_{i,j}} \sum_{r=1}^4 [\mathbf{F}, \mathbf{G}]_r^p \cdot \mathbf{n}_r \Delta L_r + \Delta t \mathbf{S}_{i,j}^p \quad (11)$$

$$\mathbf{U}_{i,j}^{n+1} = \frac{1}{2} (\mathbf{U}_{i,j}^p + \mathbf{U}_{i,j}^c) \quad (12)$$

where  $p$  and  $c$  stand for predictor and corrector values. For each side ( $r = 1, \dots, 4$ ),  $\mathbf{F}_r$  and  $\mathbf{G}_r$  are obtained referring to upstream and downstream volumes alternately. The sequence is concluded in four time steps.

Generally, second order central schemes introduce spurious oscillations. To avoid such problems, viscosity terms are added to the previous equations in order to prevent non linear instability and to dissipate numerical oscillations. Two algorithms were implemented: one proposed by Jameson and other based on the Total Variation Diminishing (TVD) properties. In particular, the last one has been preferred for its independence from any parameter. This technique is well described in the previous report.

Instead HLL scheme is an approximate Riemann solver based on the work of Harten et al. (1983) and known as the HLL Riemann solver. It is a first order accurate scheme.

This scheme applied to the two dimensional equations gives the following expression for the numerical flux across the edge of the computational cell  $\Omega_L$  on the left and  $\Omega_R$  on the right:

$$[\mathbf{f}, \mathbf{g}]_r \cdot \mathbf{n}_r = \begin{cases} [\mathbf{f}, \mathbf{g}]_L \cdot \mathbf{n}_r & \text{if } s_L \geq 0 \\ \frac{s_R([\mathbf{f}, \mathbf{g}]_L \cdot \mathbf{n}_r - s_L([\mathbf{f}, \mathbf{g}]_R \cdot \mathbf{n}_r + s_L s_R (\mathbf{U}_R - \mathbf{U}_L))}{s_R - s_L} & \text{if } s_L \leq 0 \leq s_R \\ [\mathbf{f}, \mathbf{g}]_R \cdot \mathbf{n}_r & \text{if } s_R \leq 0 \end{cases} \quad (13)$$

Equation (13) depends on the value of the wave speeds  $s_L$  and  $s_R$ , therefore it is necessary to introduce approximate expressions of these variables. The wave speed estimators used in this work are obtained by the application of the two-rarefaction Riemann solver theory (Toro, 2001):

$$s_L = \min\left([u, v]_L \cdot \mathbf{n}_r - \sqrt{gh_L}, u^* - \sqrt{gh^*}\right); s_R = \max\left([u, v]_R \cdot \mathbf{n}_r + \sqrt{gh_R}, u^* + \sqrt{gh^*}\right) \quad (14)$$

where:



$$u^* = \frac{1}{2}([u, v]_L + [u, v]_R) \cdot \mathbf{n}_r + \sqrt{gh_L} - \sqrt{gh_R}; \quad \sqrt{gh^*} = \frac{1}{2}(\sqrt{gh_L} + \sqrt{gh_R}) + \frac{1}{4}([u, v]_L - [u, v]_R) \cdot \mathbf{n}_r \quad (15)$$

Particular conditions are applied to  $s_L$  and  $s_R$  if there is a dry cell.

As for all explicit methods, both schemes have been subjected to the stability restriction given by the well-known Courant–Friedrich–Lewy (CFL) condition as follows:

$$\Delta t = C \frac{\Delta x}{\max(\sqrt{u^2 + v^2} + \sqrt{gh})} \quad (16)$$

where  $C$  is the Courant number.

In this context for the presence of low values of water depth, as those that generally characterize the rainfall runoff process in the early stage of the phenomenon, the Courant number used in these simulations is very small ranging from 0.0001 to 0.001.

The source term vector was decomposed in two different parts: the bottom variation  $\mathbf{S}_b$  written as:

$$\mathbf{S}_b = \begin{pmatrix} 0 \\ ghS_{0x} \\ ghS_{0y} \end{pmatrix} \quad (17)$$

and the friction term  $\mathbf{S}_{fr}$ :

$$\mathbf{S}_{fr} = \begin{pmatrix} 0 \\ -ghS_{fx} \\ -ghS_{fy} \end{pmatrix} \quad (18)$$

In MacCormack's scheme a technique proposed by Nujic (1995) has been introduced (Costanzo e Macchione, 2005; Costanzo e Macchione, 2004; Costanzo et al., 2002). According to Nujic, spurious oscillations are due to a wrong discretization of the momentum equations and in particular to a numerical incompatibility between the discretization of bottom variations  $ghS_{0x}$  (or  $ghS_{0y}$ ) and the pressure term  $gh^2/2$ .

The technique consists in extracting the term  $gh^2/2$  from the flux functions  $\mathbf{F}$  and  $\mathbf{G}$ , and considering it as a source term. Consequently the free surface variation along the two spatial directions substitutes the bottom variation in the source terms.

So the flux functions are modified and the terms:

$$S_{0x} = -\frac{\partial z}{\partial x}; \quad S_{0y} = -\frac{\partial z}{\partial y} \quad (19, 20)$$

are replaced with:

$$S_{Hx} = -\frac{\partial H}{\partial x}; \quad S_{Hy} = -\frac{\partial H}{\partial y} \quad (21, 22)$$

where  $H = z+h$  is water elevation and  $z$  is bed elevation.

Moreover free surface slope is discretized in a forward and backward manner according to the flux terms.

Instead in HLL scheme the bed slope is simply discretized in central manner.

Another problem concerns the wet/dry fronts, for this reason the simulation were carried on imposing a thin layer of water equal to  $10^{-4}$  m on dry cells. When the water is lower than the thin layer it has been set equal to it and the velocities are null. However, this simple treatment is not enough for overland flow simulations where water level gradients over relatively steep dry grounds occur inducing unreasonably large velocities. Then, in this work, specific treatments for calculating wet/dry fronts are also applied. In particular four typical cases presented in figure 1 have been analyzed.

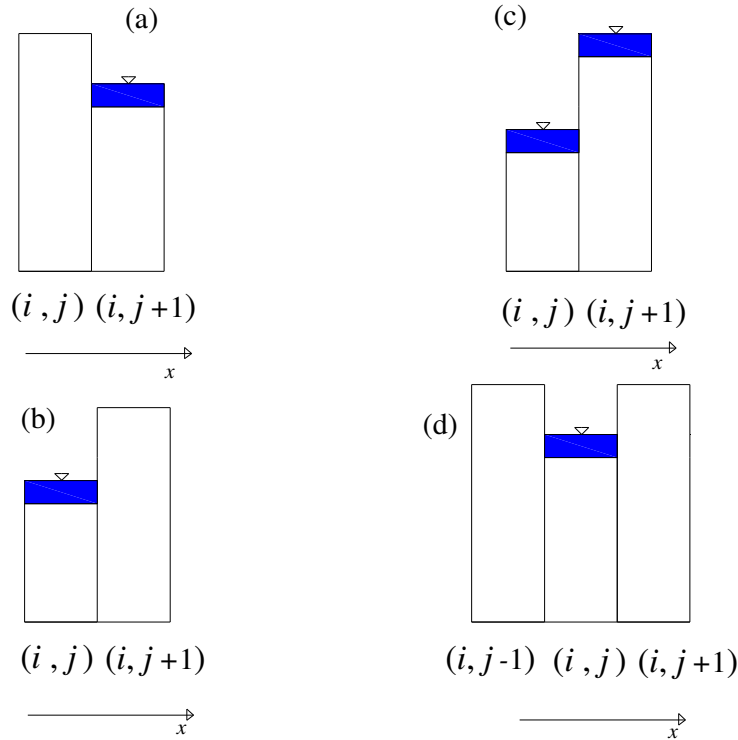


Figure 1. Wet/Dry fronts

Case a)

$$\left( z(i, j) > (z(i, j+1) + h(i, j+1)) \right), h(i, j) \leq h_{dry} \quad (23)$$

There is no exchange of mass or momentum between the cell  $(i, j)$  and the adjacent cell. In this situation, the flux terms and TVD terms are set equal to zero. The contribution of spatial variation of the free surface is also equal to zero.

Case b):

$$\left( (z(i, j) + h(i, j)) < z(i, j+1) \right), h(i, j+1) \leq h_{dry} \quad (24)$$

There is no exchange of mass or momentum between the cell  $(i, j)$  and the adjacent cell. In this situation, the flux terms and TVD terms are set equal to zero. The contribution of spatial variation of the free surface is also equal to zero.



Case c):

$$\left( (z(i, j) + h(i, j)) < z(i, j + 1) \right), h(i, j + 1) > h_{dry} \quad (25)$$

The exchange of mass is estimated instead the flux terms of momentum equations are null between the cell (i, j) and the adjacent cell. The contribution of spatial variation of the free surface is equal to zero.

Case d):

$$\left( z(i, j - 1) < (z(i, j) + h(i, j)) < z(i, j + 1) \right) \quad (26)$$

The velocity along x direction is set equal to zero and the mass conservation equation is solved only if cell (i, j-1) or cell (i, j+1) is wet.

Moreover numerical anomalies can still arise with regard to the friction term when the water depth becomes very small as it is often present in overland flow simulations. For small water depths, the friction term dominates over other terms in the momentum equations, as the term  $K^2 h^{4/3}$  appears in the denominator. In such situations it's reasonable to ignore the terms of convective inertia and the slope of the free surface in momentum equations (Liang et al. 2007). Then the momentum equations becomes:

$$\begin{aligned} \frac{\partial hu}{\partial t} &= -S_{frx} \\ \frac{\partial hv}{\partial t} &= -S_{fry} \end{aligned} \quad (27, 28)$$

where  $S_{frx}$  and  $S_{fry}$  are the components along x and y directions of the vector  $\mathbf{S}_{fr}$  (Equation 18)  
The above equations are discretized according to a partially implicit approach.

$$\frac{(hu)^{n+1} - (hu)^n}{\Delta t} = -S_{frx}^n (hu)^{n+1} \quad (29)$$

$$\frac{(hv)^{n+1} - (hv)^n}{\Delta t} = -S_{fry}^n (hv)^{n+1} \quad (30)$$

which can be re-formulated as:

$$(hu)^{n+1} = -\frac{(hu)^n}{1 + \Delta t S_{frx}^n} \quad (31)$$

$$(hv)^{n+1} = -\frac{(hv)^n}{1 + \Delta t S_{fry}^n} \quad (32)$$

In this work the Riemann solver theory is used in the description of outflow, and wall boundary conditions. The sufficient conditions imposed at the boundaries combined with equations obtained from characteristics theory give the information needed for the calculation of boundary flux as described in previous report.

## Applications

The models developed by the laboratory LAMPIT (Department of Soil Defence - University of Calabria), described above, have been applied to simulate overland flow event on real topography as showed in previous report.

In particular MacCormack's scheme was applied to simulate an overland flow event (Test 3) of an overland flow phenomenon over the Esaro basin (Calabria).

Overland flow simulations in Esaro basin has been revealed very complex due to the presence of an high irregular topography. In order to investigate the causes of numerical anomalies, we have focused the attention on a part of the basin in which numerical instabilities and other similar problems may occur for the irregularity of the surface elevation.

The analyzed domain is 2000 m x 2000 m wide and its surface elevation and contour lines are shown in figures 2 and 3. The mesh grid has a 40 m cell size.

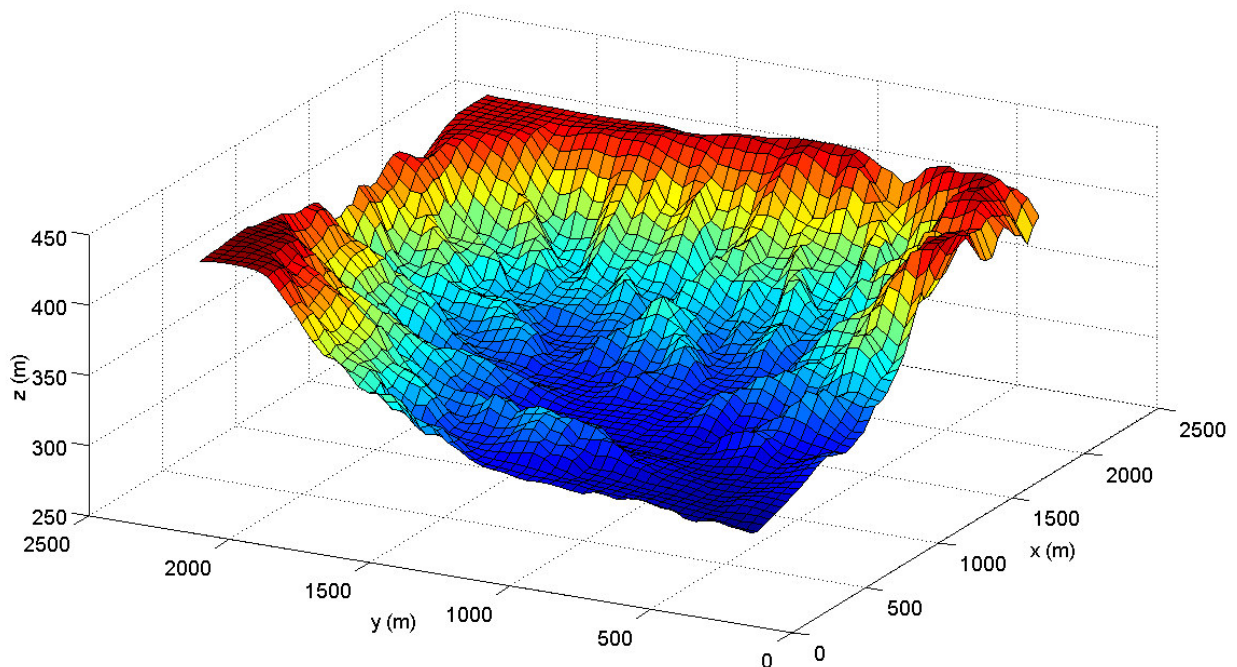
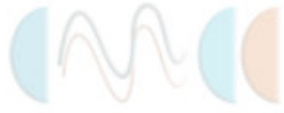


**Figure 2.** –Test 3: Surface elevation

A constant rainfall (100 mm/h) has been considered over the domain. In this simulation the TVD terms have been also introduced in the shallow water equations.

A sensibility analysis of Strickler's coefficient has been also performed for this case. Values of 5, 10, 15 and 25  $m^{1/3}/s$  have been considered as constant friction coefficient in the whole domain. In figure 4 the discharge hydrographs at the outlet of domain, obtained using different Strickler's coefficients, are shown. The phenomenon has been simulated until the hydrographs reach their



time to peak because a constant in time and space rainfall intensity (100 mm/h) has been considered.

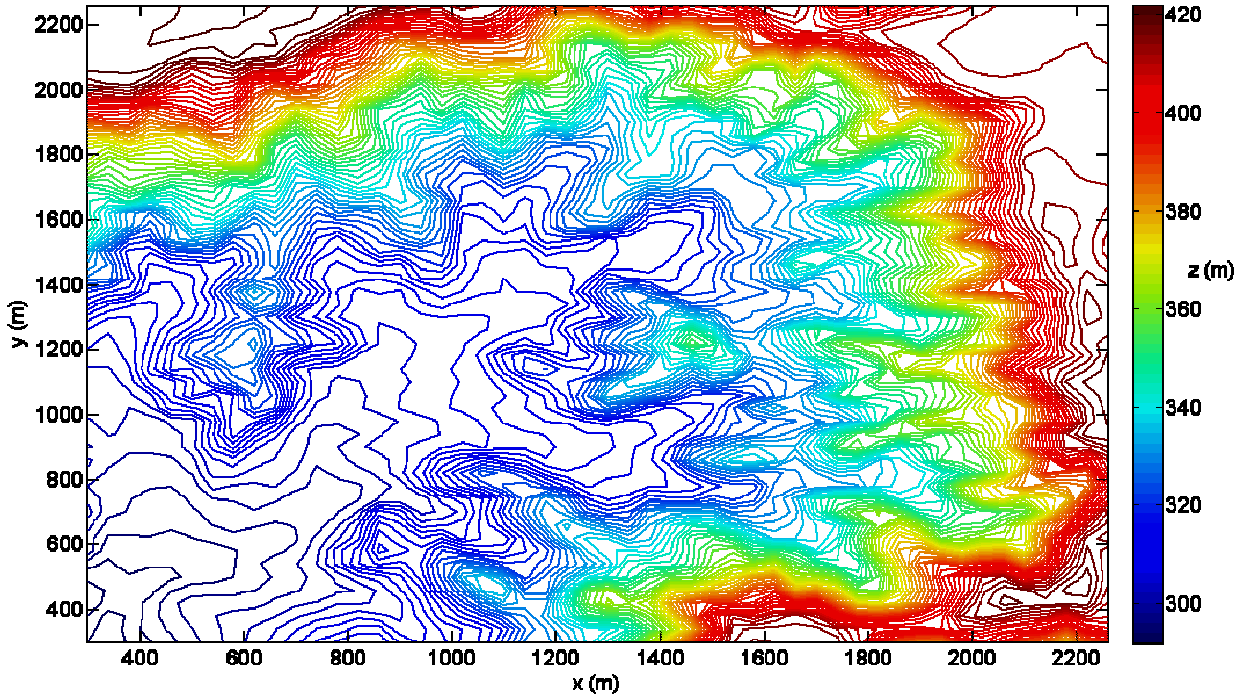


Figure 3. – Test 3: Contour lines

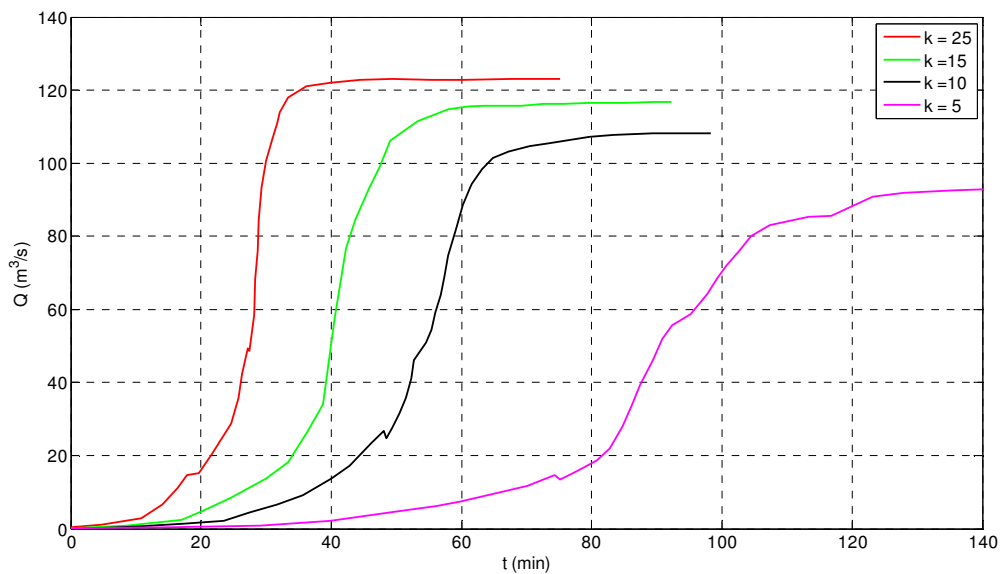
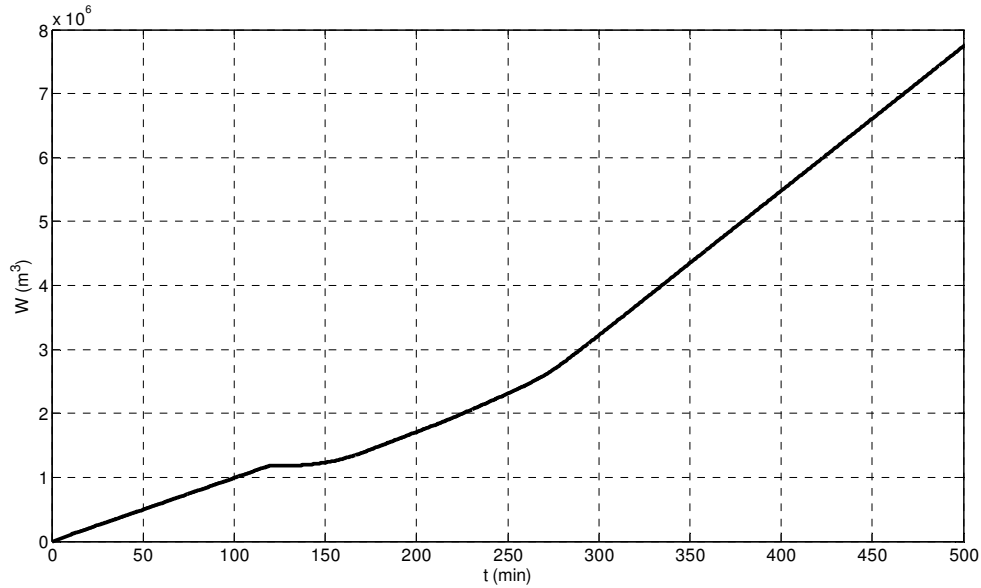


Figure 4. Test3 – Discharge Hydrographs at the channel outlet computed by MacCormack's scheme with different Stickler's coefficients  $k$  (25, 15, 10, 5  $\text{m}^{1/3}/\text{s}$ )



However in simulating the recessive limb of the flow, some numerical instability problems arise due to the presence of very low values of water depth over an irregular topography with high slope that progressively leads to the code failure. Moreover this formulation do not respect the mass conservation criterion: suddenly the volume increases and the discharge outflow rises as showed in figures 5-6 for the case of Strickler's coefficient equal to 15 in all the domain and a rainfall intensity equal to 100 mm/h for two hours. In particular figure 5 shows the computed volume obtained in each instant as sum of the volume inside the domain and that came out.



**Figure 5.** Test 3 – Computed water volume versus time

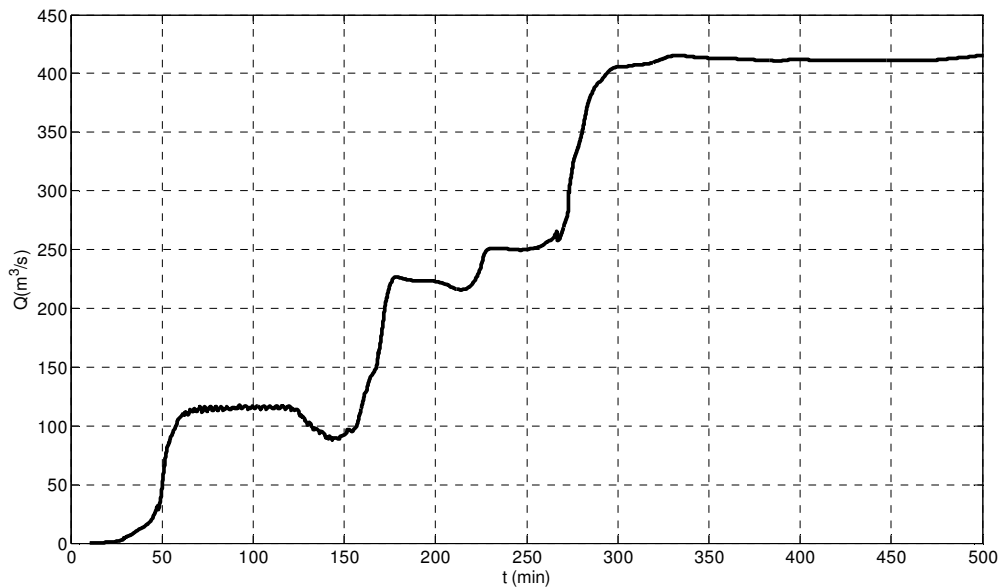


**Figure 5.** – Part of Esaro Basin – Discharge Hydrograph at the outlet of the domain due of a rainfall intensity equal to 100 mm/h for two hours



In the same way the code, based on MacCormack's scheme, has been applied to simulate an overland flow event over a topography similar to Test 2 of the previous report, with the addition of more irregularities in the central part of the domain. In previous report Test 2 concerned a propagation of a surface runoff on a domain 950 m x 1100 m; the surface elevation and the contour lines are reported in figures 7-8.

The domain has been divided according to a structured grid with different cell size (5, 20, and 40 m) and an analysis of the cell size influence on the numerical results has been performed. Also in this case the simulations refer to the propagation of surface runoff due to a constant in time and space rainfall intensity (100 mm/h and 10 mm/h). The Strickler's coefficient is constant in the whole domain ( $8 \text{ m}^{1/3}/\text{s}$ ) and the infiltration rate is set to zero. The numerical results obtained by MacCormack's scheme with different mesh size in cases of rainfall intensity equal to 100 mm/h and 10 mm/h are reported in figures 9 -10.

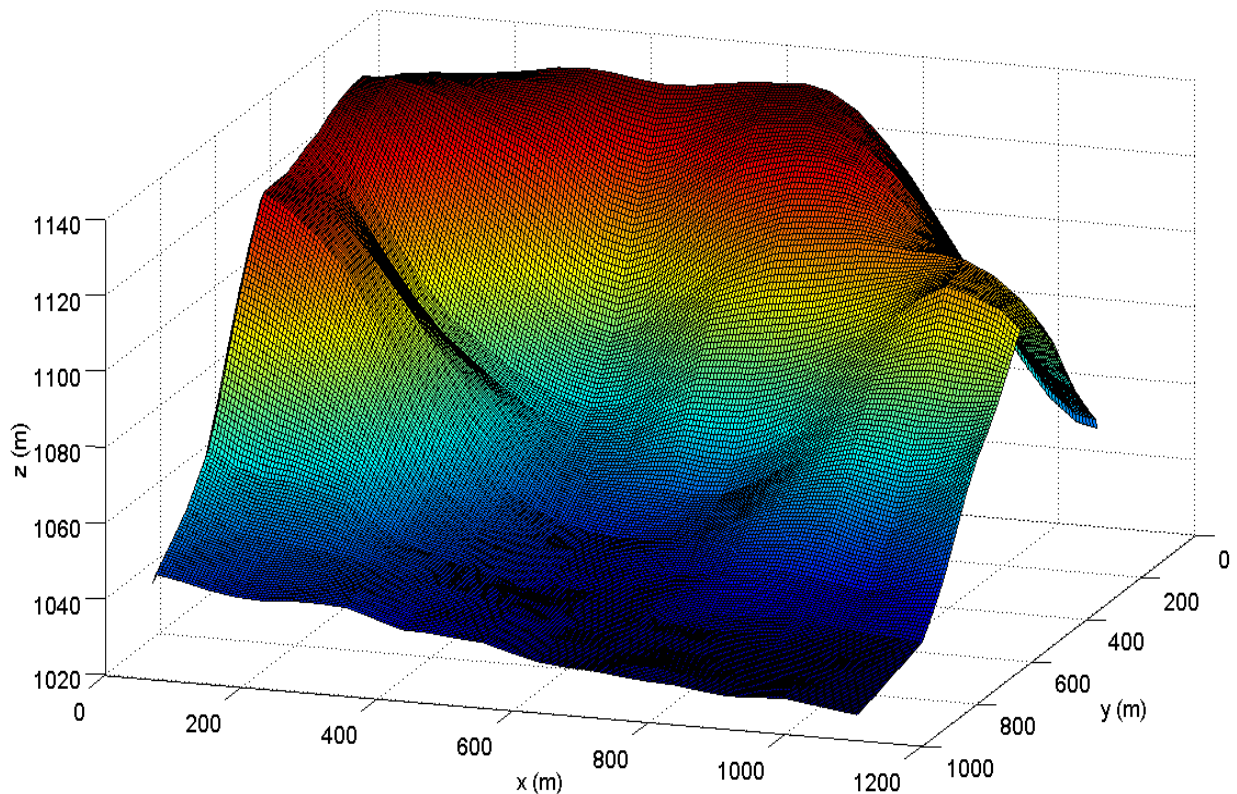


**Figure 7.** Test 2 – Surface elevation

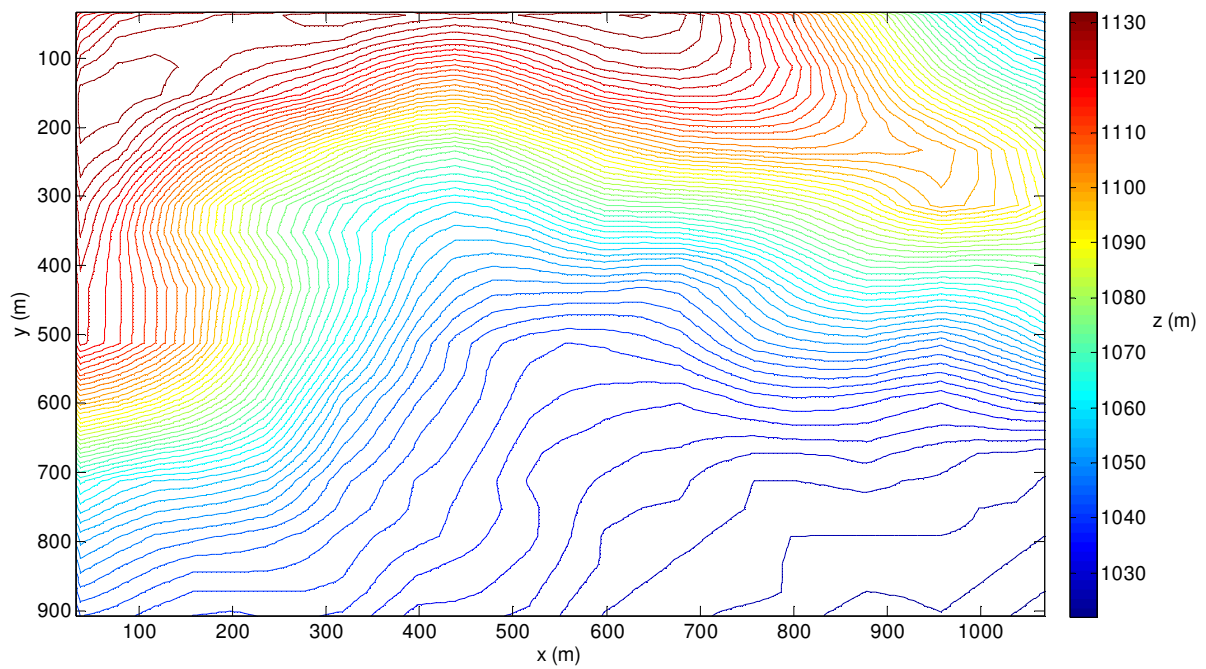


Figure 8. Test 2 – Contour lines

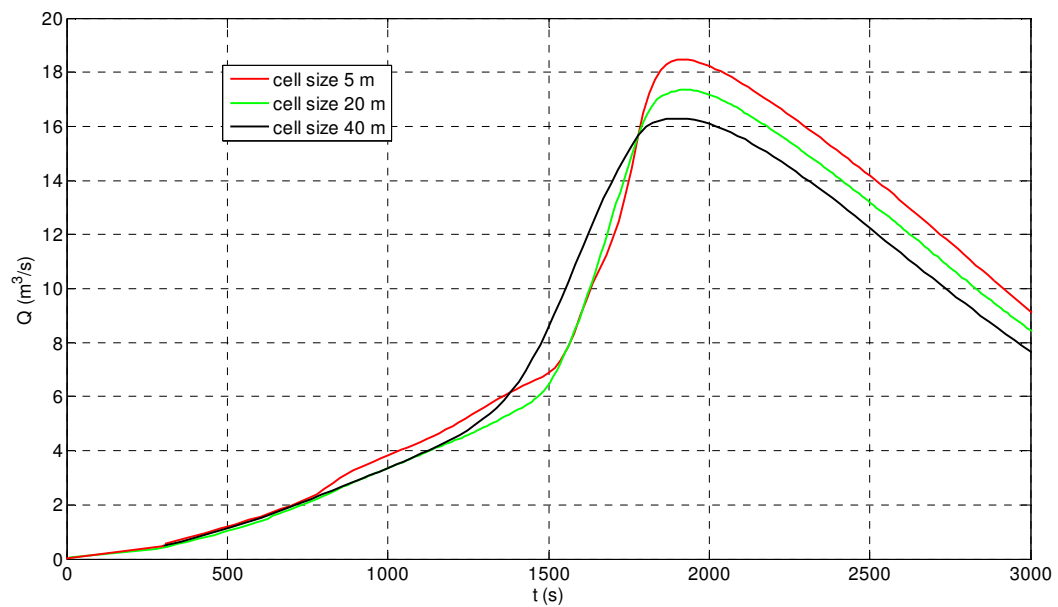
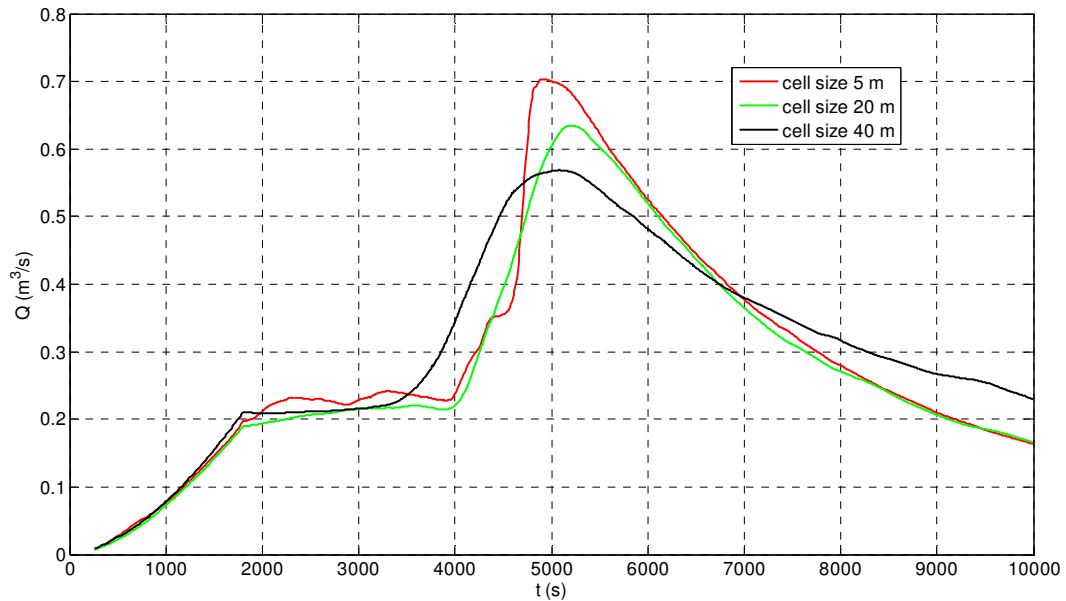


Figure 9. Test 2 – Discharge Hydrographs at the channel outlet computed using mesh size (5 m, 20 m, 40 m) with 100 mm/h rainfall intensity



**Figure 10.** Test 2 – Discharge Hydrographs at the channel outlet computed using different mesh size (5 m, 20 m, 40 m) with 10 mm/h rainfall intensity

Instead, when we simulate the propagation of the surface runoff over a more irregular topography showed in figure 11, discretized by a 40 m mesh (Test 4), in the same manner of the above test, there is a sudden volume increase, during the recession phase of the event and a rise of the discharge outflow as in figures 12-13.

All this has required a close analysis of the implemented code as reported in the next chapter.

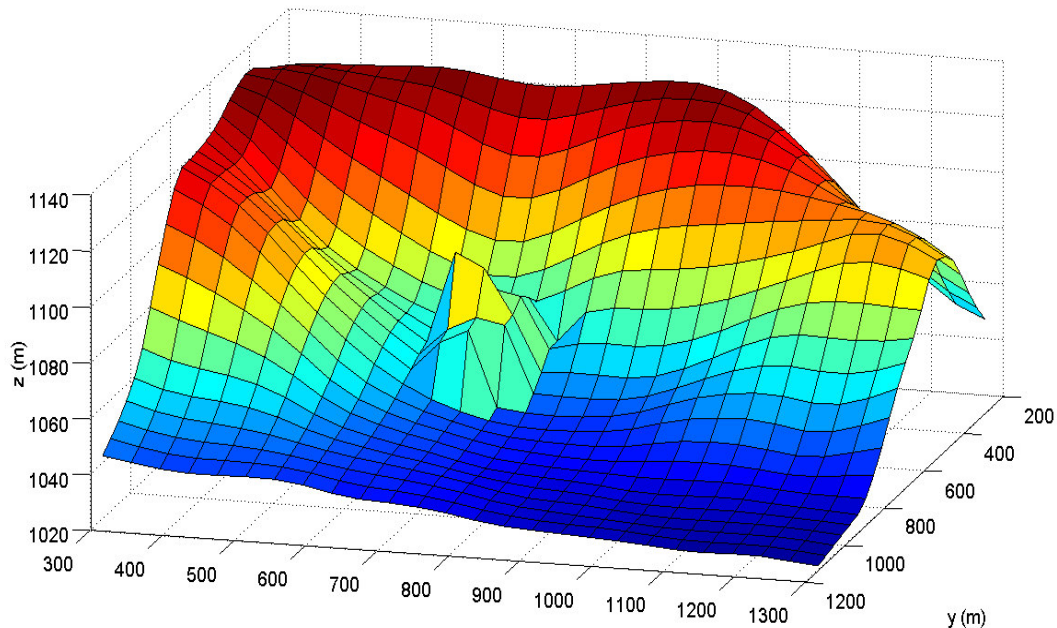


**Figure 11.** Test 4 – Surface elevation

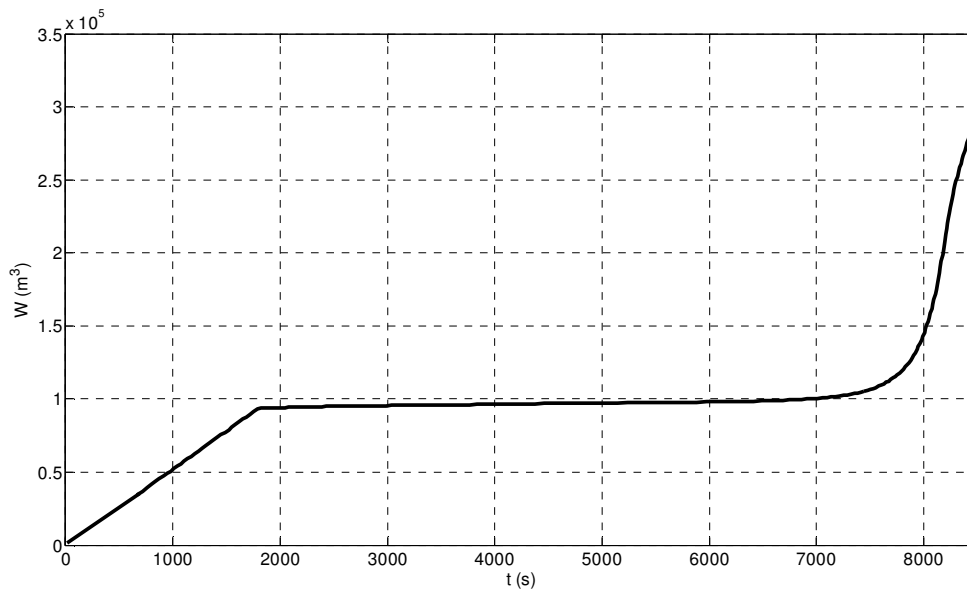


**Figure 12.** Test 4 – Computed water volume versus time

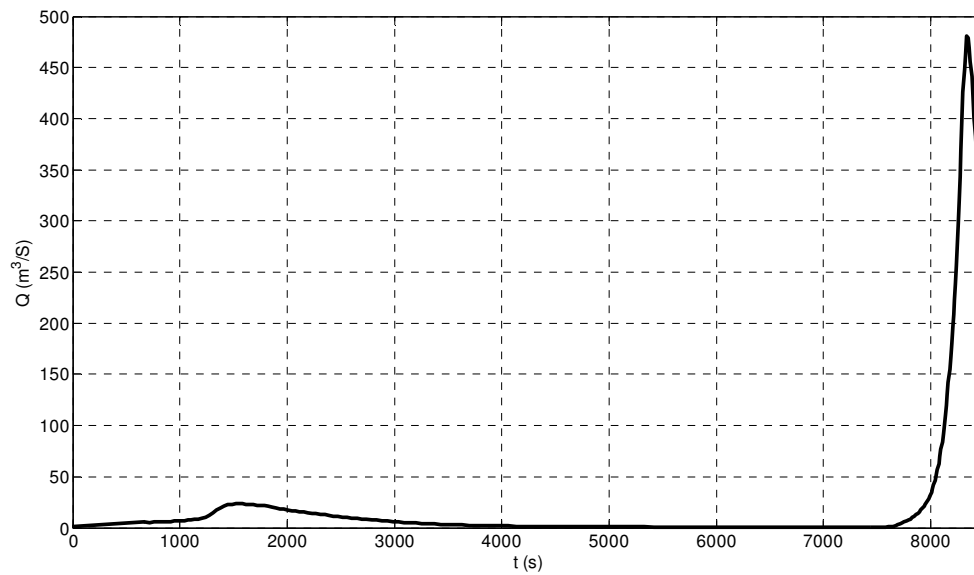


**Figure 13.** Test 4 – Discharge hydrograph at the outlet of domain



## Numerical techniques for preventing computational instability problems

Initially, to resolve the above mentioned numerical problems, a particular subroutine has been implemented by which the dry cells surrounded by other dry cells, in the absence of rain, are excluded from the computation. This allowed to avoid the calculation several times on cells with very small height of water and at the same time to reduce the threshold of the thin layer of water from  $10^{-4}$  m to  $10^{-8}$  m.

Moreover, following some articles (Brufau et al. 2004, Liang and Borthwick 2009), water added to maintain the thin layer is subtracted from the adjacent cell containing most water in order to maintain mass conservation.

To maintain the front velocity components, the conserved variables  $uh$  and  $vh$  in the adjacent cell where water has been subtracted are also modified accordingly so that  $u$  and  $v$  remain the same as before.

After a thorough bibliographic review on the specific treatment of the wet-dry fronts (Liang and Borthwick 2009; Delis et al. 2008, Aureli et al. 2008, Begnudelli and Sanders 2007, Brufau et al. 2004), we have considered the above mentioned treatments redundant, in fact the cases (a, c, d) are included in the solutions of the shallow water equations. Only the treatment of wet-dry fronts in the case (b) has been applied.

Moreover in the various simulations carried out we have realized that the conditions expressed by equations 31-32 are negligible because it is possible to apply the complete shallow water equations without simplifications of terms also to simulate the surface runoff of water heights below  $10^{-2}$  m as long as an adequately discretization of the friction term is applied as will be described below.

In fact, singularities can still arise with regard to the bed friction term when the water depth becomes very small as it is often present in overland flow simulations. For small water depths, the bed friction term dominates over other terms in the momentum equation, as the term  $K^2 h^{4/3}$  appears in the denominator.

In literature few works concern in detail the consequences of the discretization of the friction term. The most commonly and simple reported procedure is the pointwise discretization of the terms independent of the methodology used for the rest of the system. However this criterion in presence of high friction or low water depth leads to numerical instabilities. Therefore the time step reducing over the minimum value given by the CFL condition, or an implicit treatment of the pointwise discretized friction source term are needed (Liang et al., 2007; Costanzo and Macchione, 2006, Yoon & Kang, 2004; Caleffi et al., 2003). In this work this is a very evident problem due to the low values of water depths. According to Burguete et al. (2007), the technique based on the limitation of the friction term's values has been implemented in order to avoid incorrect values of the friction term in unsteady cases of advancing front over dry and rough surfaces. Given that the maximum effect of the friction force is to stop the water flow, a necessary condition in the solution is that the updated value of the unit discharge along the two spatial directions ( $hu$ ) and ( $hv$ ) at  $n+1$  time step after the addition of the discrete friction term retains the same sign of the value at the previous time level  $n$ . Then when the numerical friction force exceeds the sum of the other terms in momentum equations that leads to change the sign of the velocity, it will be limited to the maximum value and the velocity is set to zero. This technique has been applied both to predictor step and to corrector step. For example in predictor step along the  $x$  directions the momentum equation can be written as:



$$(hu)_{i,j}^p = (hu)_{i,j}^n - \frac{\Delta t}{\Omega_{i,j}} [(f_x \Delta x - g_x \Delta y)]^n + \Delta t S_{bxi,j}^n - \Delta t S_{frxi,j} \quad (33)$$

with  $f_x$  and  $g_x$  the components of the vectors  $\mathbf{F}$  and  $\mathbf{G}$  along the  $x$  direction,  $S_{bx}$  and  $S_{frx}$  the components along the same direction of the vectors  $\mathbf{S}_b$  and  $\mathbf{S}_{fr}$  (Equations .17-18)

Considering  $(hu)_{i,j}^*$  as follow:

$$(hu)_{i,j}^* = (hu)_{i,j}^n - \frac{\Delta t}{\Omega_{i,j}} [(f_x \Delta x - g_x \Delta y)]^n + \Delta t S_{bxi,j} \quad (34)$$

The condition suggested by Burguete et al. (2007), in order to don't change the versus of the velocity due to the friction term, is:

$$(hu)_{i,j}^p (hu)_{i,j}^* \geq 0 \quad (35)$$

or:

$$(hu)_{i,j}^* [(hu)_{i,j}^* - \Delta t S_{frx}] \geq 0 \text{ that implies } S_{frx} \leq \frac{(hu)^*}{\Delta t} \quad (36)$$

when the above condition is not fulfill the velocity is set equal to zero.

Moreover for small water depths also a semi-implicit approach to discretize friction terms is used.

In literature there are some different semi-implicit approach to discretize the friction term. One method (Caleffi et al. 2003, Costanzo and Macchione 2006, Aureli et al. 2008) introduces an appropriate coefficient,  $\beta$ , to weight the variables at current time step, and a coefficient  $(1 - \beta)$  to weight the variables at the previous time step; one obtains:

$$\mathbf{S}_{fr} = \beta \mathbf{S}_{fr}^{n+1} + (1 - \beta) \mathbf{S}_{fr}^n = \mathbf{S}_{fr}^n + \beta (\mathbf{S}_{fr}^{n+1} - \mathbf{S}_{fr}^n) \quad (37)$$

Moreover it's possible to develop in the time series the term  $\mathbf{S}_{fr}^{n+1}$  as follow:

$$\mathbf{S}_{fr}^{n+1} \approx \mathbf{S}_{fr}^n + \frac{\partial \mathbf{S}_{fr}}{\partial t} \Delta t = \mathbf{S}_{fr}^n + \frac{\partial \mathbf{S}_{fr}}{\partial \mathbf{U}} \frac{\partial \mathbf{U}}{\partial t} \Delta t = \mathbf{S}_{fr}^n + \mathbf{Q}_f \frac{\partial \mathbf{U}}{\partial t} \Delta t \approx \mathbf{S}_{fr}^n + \mathbf{Q}_f \Delta \mathbf{U} \quad (38)$$

where  $\mathbf{Q}_f$  is the jacobian matrix  $\partial \mathbf{S}_{fr} / \partial \mathbf{U}$ .

Then  $\mathbf{S}_{fr}$  has been discretized as follow:

$$\mathbf{S}_{fr} = \beta \mathbf{S}_{fr}^{n+1} + (1 - \beta) \mathbf{S}_{fr}^n = \mathbf{S}_{fr}^n + \beta (\mathbf{Q}_f \Delta \mathbf{U}) \quad (39)$$

Combining with the discretization of the other terms of the shallow water equations one obtains:

$$\Delta \mathbf{U} = (\mathbf{I} - \Delta t \beta \mathbf{Q}_f)^{-1} \left( -\frac{\Delta t}{\Omega_{i,j}} \sum_{r=1}^4 (\mathbf{F} \delta x - \mathbf{G} \delta y)_r^n + \mathbf{S}_{fr}^n \right) + \Delta t \mathbf{S}_{bxi,j}^n \quad (40)$$

where  $\mathbf{I}$  is the identity matrix.

Another semi-implicit approach (Fiedler and Ramirez 2000; Brufau et al. 2004; Delis et al. 2008; Burguete et al. 2008) implies the introduction of a coefficient  $\theta$  that is the implicitness degree of

the friction term discretization, for example along the  $x$  direction the term  $S_{frx} = g \frac{\sqrt{u^2 + v^2}}{K^2 h^{4/3}} (uh)$  of the equation 18 is discretized as follow:

$$\begin{aligned} \Delta t \left\{ g \frac{\sqrt{u^2 + v^2}}{K^2 h^{4/3}} \left[ \theta (uh)^n + (1 - \theta) (uh)^{n+1} \right] \right\} &= \Delta t \theta S_{frx}^n + \Delta t \left( -g \frac{\sqrt{u^2 + v^2}}{K^2 h^{4/3}} (1 - \theta) (uh)^{n+1} \right) = \\ &= \Delta t \theta S_{frx}^n + \Delta t \left( (1 - \theta) (uh)^{n+1} \frac{S_{frx}^n}{(uh)^n} \right) \end{aligned} \quad (41)$$



Combing Equation 41 with the discretization of the shallow water ones:

$$(uh)_{i,j}^{n+1} = (uh)_{i,j}^n - \frac{\Delta t}{\Omega_{i,j}} \sum_{r=1}^4 (f\delta x - g\delta y)_r^n + \Delta t S_{bx_{i,j}}^n + \Delta t \theta S_{frx_{i,j}}^n + \Delta t \left( (1-\theta)(uh)_{i,j}^{n+1} \frac{S_{frx_{i,j}}^n}{(uh)_{i,j}^n} \right) \quad (42)$$

that is:

$$(uh)_{i,j}^{n+1} \left[ 1 - (1-\theta)\Delta t \frac{S_{frx}^n}{(uh)_{i,j}^n} \right] = (uh)_{i,j}^{n+1} - \frac{\Delta t}{\Omega_{i,j}} \sum_{r=1}^4 (f\delta x - g\delta y)_r^n + \Delta t S_{bx_{i,j}}^n + \Delta t \theta S_{frx_{i,j}}^n \quad (43)$$

or rather:

$$(uh)_{i,j}^{n+1} = \frac{(uh)_{i,j}^n - \frac{\Delta t}{\Omega_{i,j}} \sum_{r=1}^4 (f\delta x - g\delta y)_r^n + \Delta t S_{bx_{i,j}}^n + \Delta t \theta S_{frx_{i,j}}^n}{1 - (1-\theta)\Delta t \frac{S_{frx_{i,j}}^n}{(uh)_{i,j}^n}} \quad (44)$$

The two different semi-implicit approaches to discretize the friction term have been applied obtaining similar results so the last described approach has been preferred for its simple implementation that avoids the computation of the jacobian matrix.

The above mentioned implemented numerical techniques have allowed to avoid the numerical instabilities due to the presence of low values of water and to simulate the recession limb of the discharge hydrographs until the end of the phenomenon.

Then the code has been applied to simulate the surface runoff over the domain more complex (figure 11) than that of the test 2 of the previous report (figure 7). The rainfall intensity is equal to 10 mm/h for  $t=1800$  s. The numerical results in terms of water volume and the discharge hydrograph at the outlet of the domain are showed in figures 14-15. In particular figure 14 shows the computed water volume obtained using MacCormack and HLL schemes in each instant as sum of the water volume inside the domain and that came out and the rainfall volume. The mass conservation criterion is fulfilled as the two lines are very similar.

In figures (14-15) the results obtained by the first order HLL scheme are also reported. The schemes respect mass conservation and simulates the recession limb of the discharge hydrograph until the end of the event. Moreover, as might be expected, the numerical result obtained by HLL scheme is more diffusive and it shows a lower peak.

Successively the implemented codes have been applied to simulate the Test 3 of a overland flow over a part of Esaro Basin (figures 2-3), and the above described numerical techniques made it possible to avoid the numerical oscillations that appeared before. In the same context, sensitivity analysis, to vary the Courant number ( $10^{-3}$  and  $10^{-4}$ ) and the value of the thin layer of the water depth (from  $10^{-8}$  m to  $10^{-5}$  m), has been made.

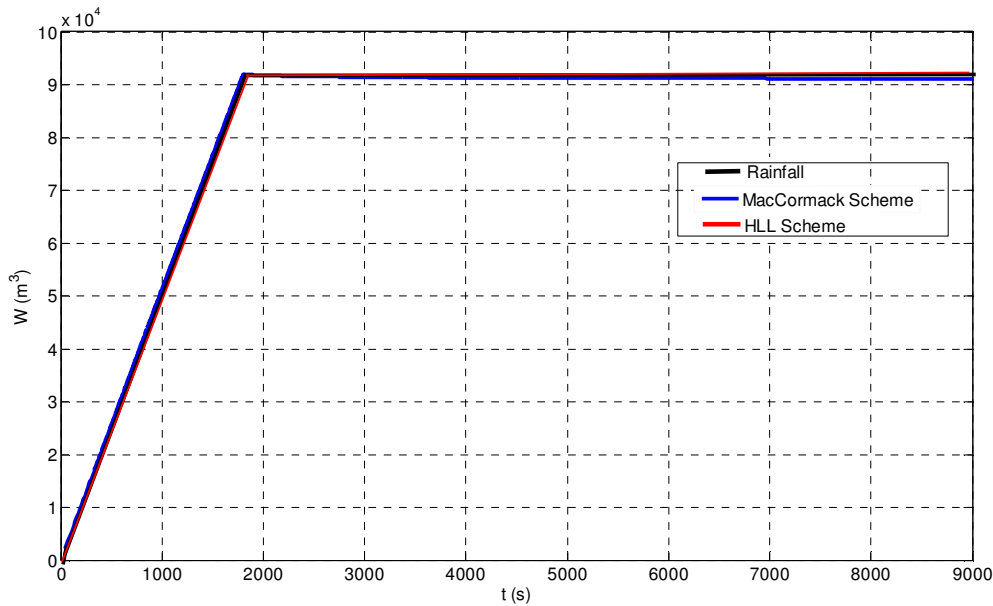


**Figure 14.** Test 4 – Comparison between computed water volume and rainfall volume versus time

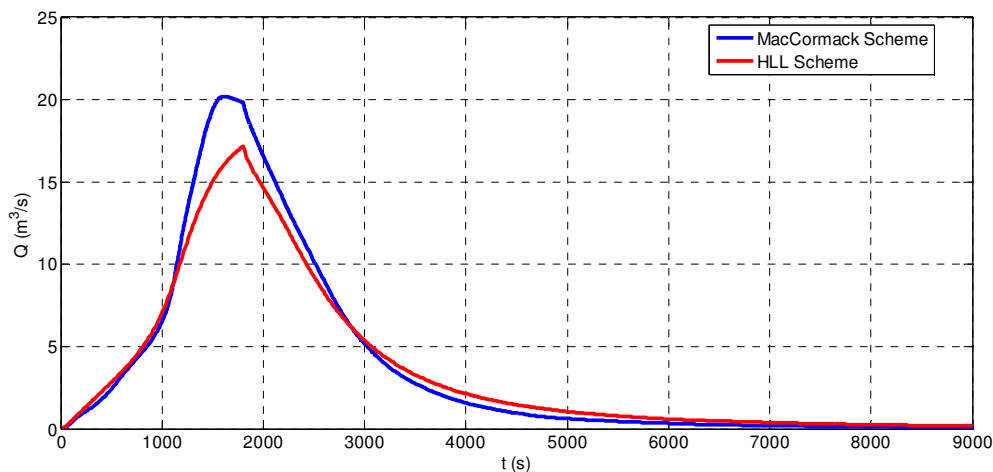


**Figure 15.** Test 4 – Discharge hydrographs at the outlet of domain computed by MacCormack Scheme and HLL Scheme

For MacCormack's scheme, in the case of rainfall intensity equal to 100 mm/h, the differences in terms of water volume are very small varying the thin value of water depth considering a Courant number equal to  $10^{-3}$  as in figures 16-17. The same results are obtained assuming a Courant number of  $10^{-4}$ .

Instead in the simulation of the surface runoff due to a lower rainfall intensity equal to 10 mm/h, the numerical results are more affected by the value of Courant number and by the thin water depth as it is showed in figures 18-21. In particular figures 18 and 20 show the comparison between the computed water volume and rainfall volume versus time assuming a Courant number equal to  $10^{-3}$  (figure 18) and a Courant number of  $10^{-4}$  (figure 20) varying the thin layer of water. Instead figures 19 and 21 represent the discharge hydrographs at the end of the domain with the



same assumptions. The mass conservation error and, in the same manner, the differences of discharge values at the outlet, are dependent on the thin layer value of water depth that it almost becomes a calibration parameter. All this probably is due to the presence of very low water depths that much affected the results obtained by the scheme. All this will be a further aspect of the study in order to reduce these differences.

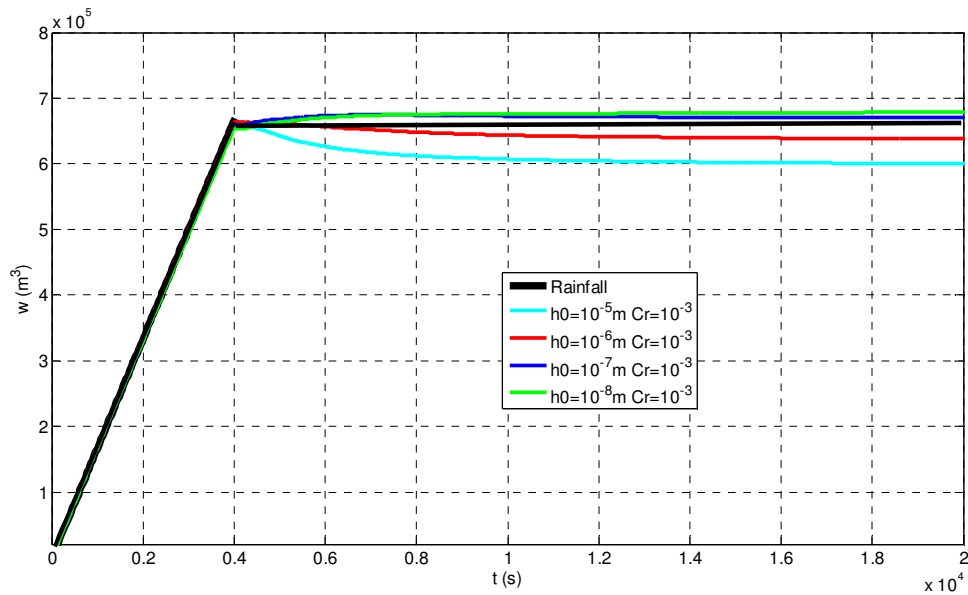


**Figure 16.** Test 3 – Comparison between rainfall volume and computed water volume versus time using Courant number  $10^{-3}$  and varying the thin layer of water (rainfall intensity = 100 mm/h, MacCormack's scheme)

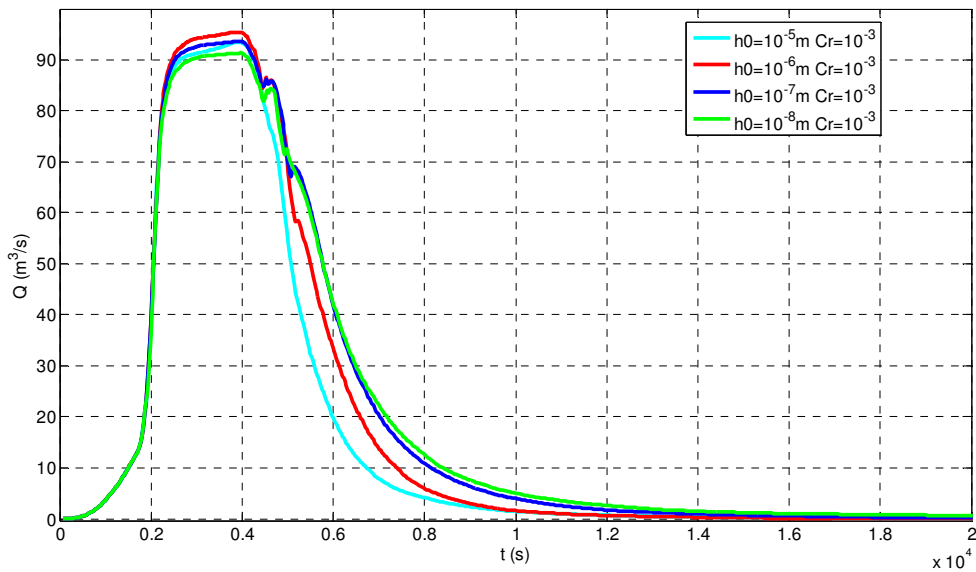


**Figure 17.** Test 3 – Discharge hydrographs at the outlet of domain assuming a Courant number  $10^{-3}$  and varying the thin water layer (rainfall intensity = 100 mm/h, MacCormack's scheme)

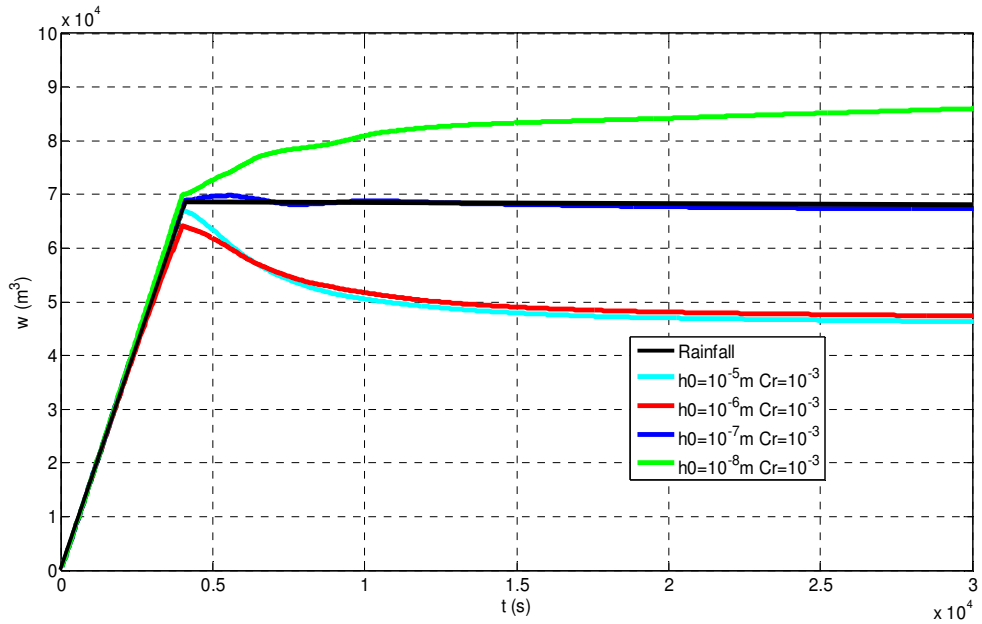


**Figure 18.** Test 3 – Comparison between rainfall volume and computed water volume versus time using Courant number  $10^{-3}$  and varying the thin layer of water (rainfall intensity = 10 mm/h, MacCormack's scheme)

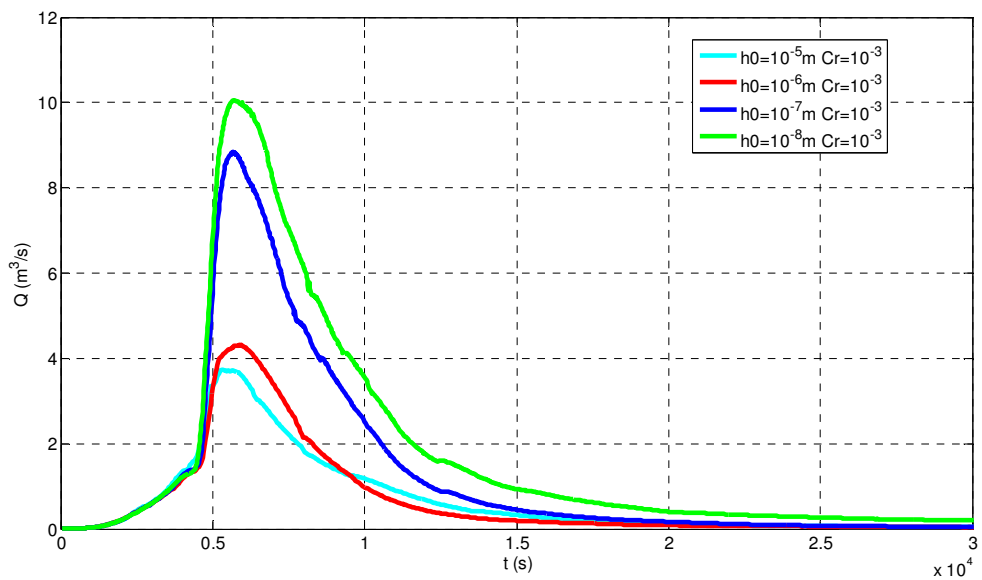


**Figure 19.** Test 3 – Discharge hydrographs at the outlet of domain assuming a Courant number  $10^{-3}$  and varying the thin water layer (rainfall intensity = 10 mm/h, MacCormack's scheme)

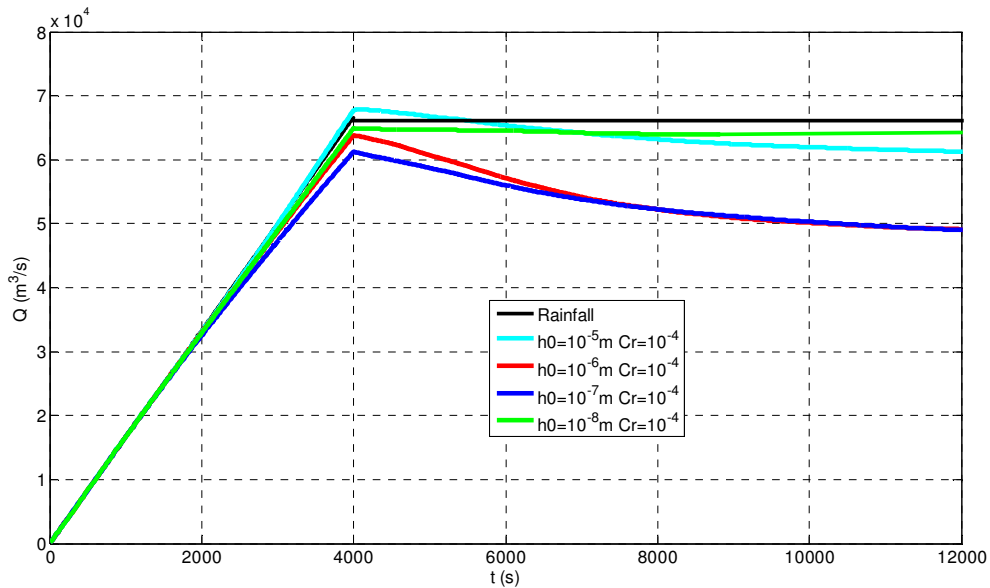


**Figure 20.** Test 3 – Comparison between rainfall volume and computed water volume versus time using Courant number  $10^{-4}$  and varying the thin layer of water (rainfall intensity = 10 mm/h, MacCormack’s scheme)

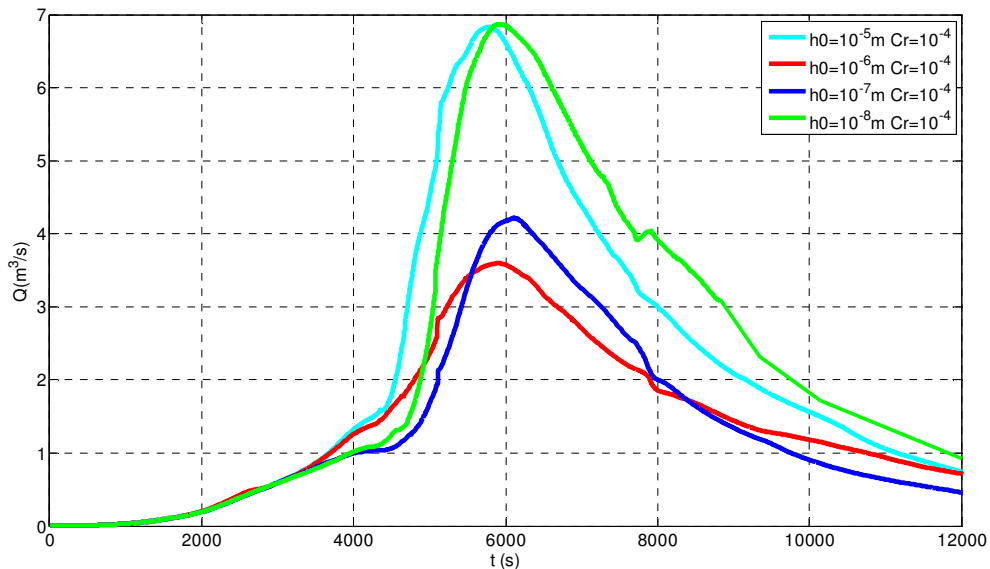


**Figure 21.** Test 3 – Discharge hydrographs at the outlet of domain assuming a Courant number  $10^{-4}$  and varying the thin water layer (rainfall intensity = 10 mm/h, MacCormack’s scheme)

The same numerical analysis has been made using HLL scheme. Also this scheme well simulate the whole event and the recession limb of the discharge hydrograph without numerical instabilities. Moreover, unlike MacCormack scheme, also in the case of rainfall intensity equal to 10 mm/h, the mass conservation is fulfilled and there are no differences in terms of water volume and discharge varying the thin value of water depth considering a Courant number equal to  $10^{-4}$  as in figures 22-23.

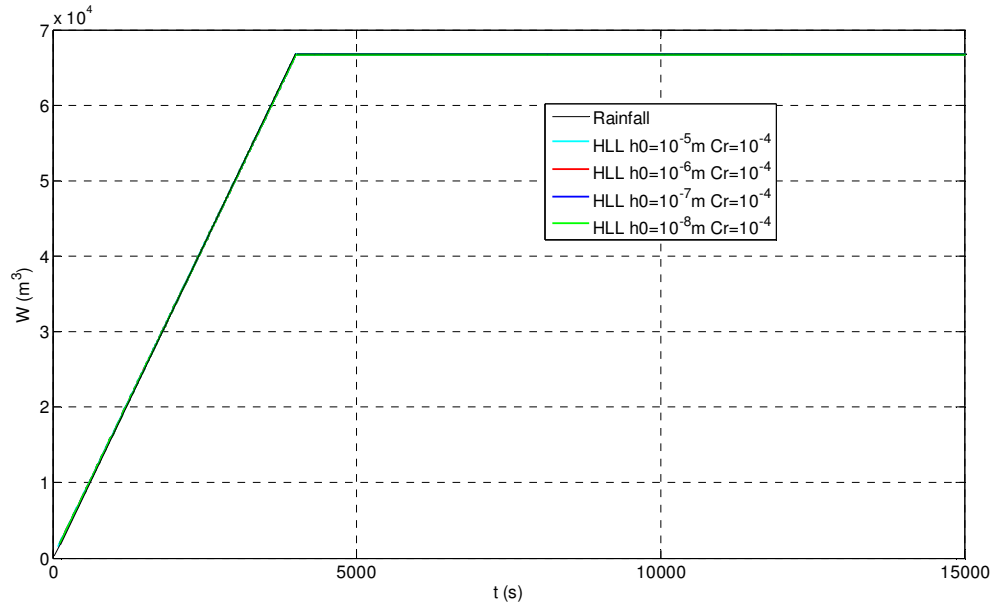


**Figure 22.** Test 3 – Comparison between rainfall volume and computed water volume versus time using Courant number  $10^{-4}$  and varying the thin layer of water (rainfall intensity = 10 mm/h, HLL scheme)

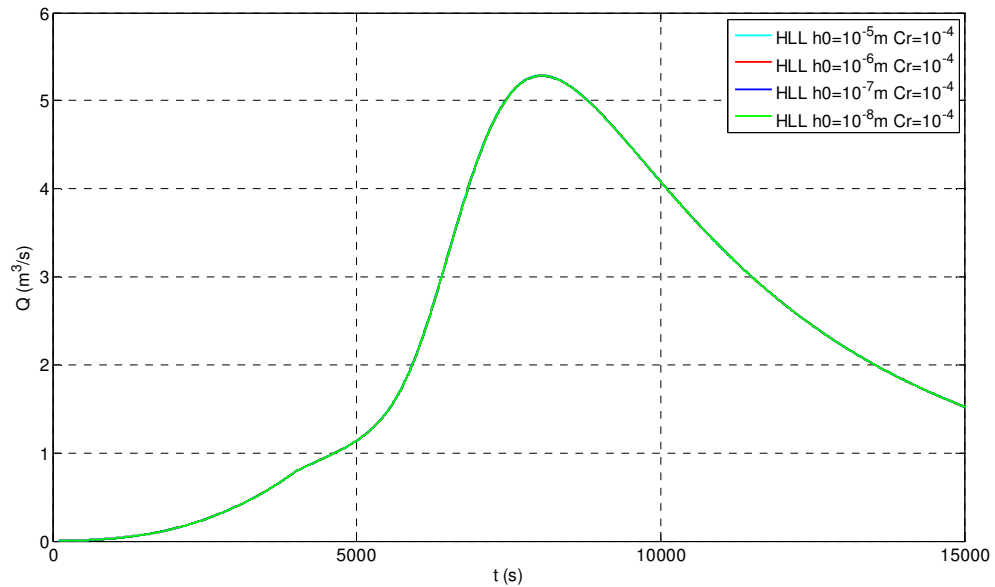


**Figure 23.** Test 3 – Discharge hydrographs at the outlet of domain assuming a Courant number  $10^{-4}$  and varying the thin water layer (rainfall intensity = 10 mm/h, HLL scheme)



## CONCLUSIONS

In this report, according to a comparative analysis on numerical schemes, the MacCormack's scheme and HLL have been improved and some numerical techniques have been implemented in order to simulate real overland flow situations.

This has been a difficult task because of the presence of small water depths over high slope and irregular topography that may induce numerical anomalies.

To avoid these problems some numerical techniques have been implemented such as the addition of further terms according to the TVD property in MacCormack's scheme, a particular discretization of the source terms and specific treatments for calculating wet dry fronts have been also applied in both schemes.

Initially, to resolve the numerical problems, a particular subroutine has been implemented by which the dry cells surrounded by other dry cells, in the absence of rain, are excluded from the computation. Successively, after a thorough bibliographic review on the specific treatment of the wet-dry fronts, a numerical technique to simulate also these situations has been applied. Moreover in order to maintain mass conservation the water added to maintain the thin layer is subtracted from the adjacent cell containing most water.

With regard to the friction term, two semi implicit approaches have been analyzed and applied in order to avoid numerical instabilities due to the presence of very low water depth.

The analyzed code has been applied to simulate a surface runoff over a domain more complex than that of the Test 2 of the previous report. The simulation well fulfils the mass conservation property until the end of the event and the recession limb of the outlet discharge is correctly calculated. Then the codes have been applied to the propagation of the surface runoff over a part of the Esaro Basin. In this context a sensitivity analysis, to vary the Courant number and the value of the thin layer of the water depth, has been made.

For both schemes, in case of rainfall intensity equal to 100 mm/h, the differences in terms of discharge and mass conservation are very small varying both the Courant number and the thin value of water depth.

In the simulation, instead, of the surface runoff due to a lower rainfall intensity equal to 10 mm/h, the numerical results, obtained by MacCormack's scheme, are more affected by the value of Courant number and by the thin water depth. All this probably is due to the presence of very low water depth and it will be a further aspect of the study in order to reduce these differences. Instead HLL scheme, also in the case of rainfall intensity equal to 10 mm/h, fulfils the mass conservation and there are no differences in terms of water volume and discharge varying the thin value of water depth.

## References

- Aureli F.; Maranzoni A.; Mignosa P. and Ziveri C. (2008). "Dam-Break Flows: Acquisition of Experimental Data through an Imaging Technique and 2D Numerical Modeling". *Journal of Hydraulic Engineering*, Vol. 134, No. 8: 1089–1101.
- Begnudelli L. and Sanders B. F. (2007). "Conservative Wetting and Drying Methodology for Quadrilateral Grid Finite-Volume Models". *Journal of Hydraulic Engineering*, Vol. 133, No. 3: 312–322.
- Brufau P., García Navarro P. and Vazquez-Cendon M. E. (2004). "Zero mass error using unsteady wetting–drying conditions in shallow flows over dry irregular topography".



- International Journal of Numerical Method in Fluids*, 45:1047–1082, John Wiley & Sons Ltd.¶
- Burguete J., García-Navarro P., Murillo J. (2008). “Friction term discretization and limitation to preserve stability and conservation in the 1D shallow-water model: Application to unsteady irrigation and river flow.” *International Journal for Numerical Methods in Fluids* 58: 403–425
- Burguete, J, García-Navarro P., Murillo J. and García-Palacín I. (2007). “Analysis of the friction term in the one-dimensional shallow water model”. *Journal of Hydraulic Engineering* 133(9), 1048-1063.
- Caleffi V., Valiani A., Zanni A. (2003). “Finite volume method for simulating extreme flood events in natural channels”. *Journal of Hydraulic Research*, vol. 41 (2): 167-177.
- Fiedler, F. R., Ramirez, J. A. (2000). “A numerical method for simulating discontinuous shallow flow over an infiltrating surface”. *International Journal of Numerical Method in Fluids*, 32: 219-240, John Wiley & Sons Ltd.
- Costanzo, C., Macchione F. (2004). “Prestazioni di alcuni schemi bidimensionali ai volumi finiti per problemi di dam break”. Proceedings of the *XXIX Convegno di Idraulica e Costruzioni Idrauliche*, Trento, 2004, Ed. Bios:Cosenza, 2004, 1: 829-836.
- Costanzo, C., Macchione, F. (2005). “Comparison of two-dimensional finite volume schemes for dam break problem on an irregular geometry”. Proceedings of the *XXXI IAHR Congress*, Seoul, Korea 2005, Theme D, 3372-3381. CD-ROM.
- Costanzo C., Macchione F. (2006). “Tecniche numeriche per la simulazione della propagazione di piene su fondo irregolare”. Proceedings of *Tecniche per la Difesa dall’Inquinamento*, G. Frega (a cura di), Editoriale Bios, Cosenza, 2006, Vol. 26 : 423-440.
- Costanzo, C., Macchione F. (2006). “Modelli di simulazione dei fenomeni di allagamento in zona urbana: applicazione ad un caso reale”. Proceedings of the *XXX Convegno di Idraulica e Costruzioni Idrauliche - IDRA2006*, Roma, 10 - 15 settembre, 2006, Casa Editrice Università degli Studi di Roma La Sapienza, CD-ROM.
- Delis A.I., Kazolea M. and Kampanis N. A. (2008). “A robust high-resolution finite volume scheme for the simulation of long waves over complex domains”. *International Journal for Numerical Methods in Fluids* 56:419–452.
- Fiedler F. R., Ramirez J. A. (2000). “A numerical method for simulating discontinuous shallow flow over an infiltrating surface”. *International Journal for Numerical Methods in Fluids* (32) : 219–240
- Harten A., Lax P., van Leer B., 1983. On upstream differencing and Godunov-type schemes for hyperbolic conservation laws. *SIAM Review*, 25: 35-61.
- Hirsch C., 1990. *Numerical computation of internal and external flows*. John Wiley e Sons.
- Liang, D., Binliang L., Falconer R.A. (2007). “Simulation of rapidly varying flow using an efficient TVD–MacCormack scheme”. *International Journal for Numerical Methods in Fluids* 53, 811–826.
- Liang Q. and Borthwick A. G.L. (2009). “Adaptive quadtree simulation of shallow flows with wet–dry fronts over complex topography”. *Computers & Fluids* 38: 221–234.



- Nujic, M. (1995). "Efficient implementation of non-oscillatory schemes for the computation of free-surface flows". *Journal of Hydraulic Research*, 33(1), 101-111.
- Toro E.F., 2001. *Shock –Capturing Methods for Free Surface Shallow Flows*. Wiley, Chichester.
- Yoon T. H., Kang S. K. (2004). "Finite volume model for two-dimensional shallow water flows on unstructured grids". *Journal of Hydraulic Engineering*, ASCE, vol. 130 (7), pp. 678-688.